Human Reproduction, Vol.35, No.12, pp. 2793–2807, 2020
Advance Access Publication on December 1, 2020 doi:10.1093/humrep/deaa246

human reproduction

ORIGINAL ARTICLE *Reproductive Biology*

In vitro differentiation of theca cells from ovarian cells isolated from postmenopausal women

P. Asiabi[1], M.M. Dolmans[1,2], J. Ambroise[3], A. Camboni[1], and C.A. Amorim[1,*]

[1]Pôle de Recherche en Gynécologie, Institut de Recherche Expérimentale et Clinique, Université Catholique de Louvain, Brussels, Belgium [2]Gynecology and Andrology Department, Cliniques Universitaires Saint-Luc, Brussels, Belgium [3]Centre de Technologies Moléculaires Appliquées, Institut de Recherche Expérimentale et Clinique, Université Catholique de Louvain, Brussels, Belgium

*Correspondence address. Pôle de Recherche en Gynécologie, Institut de Recherche Expérimentale et Clinique, Université Catholique de Louvain, Avenue Mounier 52, bte B1.52.02, 1200 Brussels, Belgium. Tel: +32-(0)2-764-5287; E-mail: christiani.amorim@uclouvain.be

Submitted on May 5, 2020; resubmitted on July 22, 2020; editorial decision on August 25, 2020

STUDY QUESTION: Can human theca cells (TCs) be differentiated *in vitro*?

SUMMARY ANSWER: It is possible to differentiate human TCs *in vitro* using a medium supplemented with growth factors and hormones.

WHAT IS KNOWN ALREADY: There are very few studies on the origin of TCs in mammalian ovaries. Precursor TCs have been described in neonatal mice ovaries, which can differentiate into TCs under the influence of factors from oocytes and granulosa cells (GCs). On the other hand, studies in large animal models have reported that stromal cells (SCs) isolated from the cortical ovarian layer can also differentiate into TCs.

STUDY DESIGN, SIZE, DURATION: After obtaining informed consent, ovarian biopsies were taken from eight menopausal women (53–74 years of age) undergoing laparoscopic surgery for gynecologic disease not related to the ovaries. SCs were isolated from the ovarian cortex and *in vitro* cultured for 8 days in basic medium (BM) (G1), enriched with growth factors, FSH and LH in plastic (G2) or collagen substrate without (G3) or with (G4) a GC line.

PARTICIPANTS/MATERIALS, SETTING, METHODS: To confirm TC differentiation, relative mRNA levels for LH receptor (*Lhr*), steroidogenic acute regulatory protein (*Star*), cholesterol side-chain cleavage enzyme (*Cyp11a1*), cytochrome P450 17A1 (*Cyp17a1*), hydroxy-delta-5-steroid dehydrogenase, 3 beta- and steroid delta-isomerase 1 (*Hsd3b1*) and hydroxy-delta-5-steroid dehydrogenase, 3 beta- and steroid delta-isomerase 2 (*Hsd3b2*) were assessed. Immunohistochemistry was also performed for their protein detection and a specific marker was identified for TCs (aminopeptidase-N, CD13), as were markers for theca and small luteal cells (dipeptidyl peptidase IV (CD26) and Notch homolog 1, translocation-associated (NOTCH1)). Finally, we analyzed cell ultrastructure before (Day 0) and after *in vitro* culture (Day 8), and dehydroepiandrosterone (DHEA) and progesterone levels in the medium using transmission electron microscopy (TEM) and ELISA, respectively.

MAIN RESULTS AND THE ROLE OF CHANCE: Results obtained from qPCR showed a significant increase ($P < 0.05$) in mRNA levels of *Lhr* in F2 (floating cells in G2) and G4, *Cyp17a1* in G1 and F1 (floating cells in G1) and *Hsd3b2* in G1, G2, G3 and G4. Immunohistochemistry confirmed expression of each enzyme involved in the steroidogenic pathway at the protein stage. However, apart from G1, all other groups exhibited a significant ($P < 0.05$) rise in the number of CD13-positive cells. There was also a significant increase ($P < 0.05$) in NOTCH1-positive cells in G3 and G4. Ultrastructure analyses by TEM showed a distinct difference between groups and also versus Day 0. A linear trend with time revealed a significant gain ($q < 0.001$) in DHEA concentrations in the medium during the culture period in G1, G2, G3 and G4. It also demonstrated a statistical increase ($q < 0.001$) in G2, G3 and G4 groups, but G1 remained the same throughout culture in terms of progesterone levels.

LARGE SCALE DATA: N/A

LIMITATIONS, REASONS FOR CAUTION: Shorter periods of *in vitro* culture (e.g. 2, 4 and 6 days) could have led to increased concentrations of differentiated TCs in G2, G3 and G4. In addition, a group of cells cultured in BM and accompanied by COV434 cells would be necessary to understand their role in the differentiation process. Finally, while our results demonstrate that TCs can be differentiated *in vitro* from cells isolated from the cortical layer of postmenopausal ovaries, we do not know if these cells are differentiated

from a subpopulation of precursor TCs present in ovarian cortex or ovarian SCs in general. It is therefore necessary to identify specific markers for precursor TCs in human ovaries to understand the origin of these cells.

WIDER IMPLICATIONS OF THE FINDINGS: This is a promising step toward understanding TC ontogenesis in the human ovary. Moreover, *in vitro*-generated human TCs can be used for studies on drug screening, as well as to understand TC-associated pathologies, such as androgen-secreting tumors and polycystic ovary syndrome.

STUDY FUNDING/COMPETING INTEREST(S): This study was supported by grants from the Fonds National de la Recherche Scientifique de Belgique (FNRS) (C.A.A. is an FRS-FNRS Research Associate; grant MIS #F4535 16 awarded to C.A.A.; grant 5/4/150/5 awarded to M.M.D.; grant ASP-RE314 awarded to P.A.) and Foundation Against Cancer (grant 2018-042 awarded to A.C.). The authors declare no competing interests.

Key words: progenitor theca cells / human ovary / stromal cells / theca cells / cell differentiation / luteal cells

Introduction

While theca cells (TCs) play a pivotal role in follicle development and production of female steroids, they have never been studied as comprehensively as granulosa cells (GCs). Indeed, Young and McNeilly (2010) called them 'the forgotten cells of the ovarian follicle'. The theca compartment is formed during the early stages of follicle growth, surrounding the outer part of the basement membrane. It is divided into two specific layers, namely theca interna cells (TICs), which synthesize steroid hormones together with GCs, and theca externa cells, which are important during ovulation (Edson *et al.*, 2009). Recently, recruitment and differentiation of TCs were investigated in different animal models (Vitt *et al.*, 2000; Orisaka *et al.*, 2006; Honda *et al.*, 2007; Itami *et al.*, 2011; Qiu *et al.*, 2013; Liu *et al.*, 2015; Adib and Valojerdi, 2017). In mice, a subpopulation of cells known as progenitor TCs was reported to differentiate into TCs (Honda *et al.*, 2007). On the other hand, in goats and cows, studies revealed that TCs can be converted from ovarian cortical stromal cells (SCs) (Orisaka *et al.*, 2006; Qiu *et al.*, 2013, 2014). In both cases, the differentiation process was shown to be regulated by factors secreted by GCs and the oocyte (Orisaka *et al.*, 2006; Honda *et al.*, 2007; Itami *et al.*, 2011; Qiu *et al.*, 2013).

In human ovaries, TC ontogeny remains unclear. Dalman *et al.* (2018a,b) described a population of theca stem cells in the theca layer of small antral follicles that has the ability to differentiate into progenitor TCs, as well as adipocyte-, osteocyte-, chondrocyte- and oocyte-like cells. Similarly to Adib and Valojerdi (2017), Dalman *et al.* (2018a,b) collected these cells from small antral follicles, but we do not know if human TCs originate from these stem cells.

In the present study, we identified a population of TCs after *in vitro* culture of cells isolated from the cortical layer of postmenopausal human ovaries. In order to obtain TCs, we attempted to mimic the *in vivo* differentiation process by employing different growth factors (Honda *et al.*, 2007; Liu *et al.*, 2015) and adding companion GCs (Orisaka *et al.*, 2006; Qiu *et al.*, 2013). The resulting TCs closely resembled their ovarian counterparts when investigated by immunohistochemical, ultrastructural and functional analyses.

Materials and methods

Source of ovaries and ethical approval

Ovarian biopsies were taken from eight menopausal women (53–74 years of age) undergoing laparoscopic surgery for gynecologic disease not related to the ovaries, after obtaining informed consent. None of the patients were under hormone replacement therapy. Use of human ovarian tissue was approved by the Institutional Review Board of the Université Catholique de Louvain on 13 May 2019 (IRB reference 2012/23MAR/125, registration number B403201213872). The biopsies were immediately transported on ice to the laboratory in Dulbecco's modified Eagle's medium/Ham's nutrient mixture F-12 with 1% (v/v) l-alanyl-l-glutamine (DMEM/F-12 (1:1) (1X) + GlutaMAX-I; Gibco, Thermo Fisher Scientific, Merelbeke, Belgium). Once in the laboratory, the medullary part of the tissue was removed with scissors and the epithelial layer was carefully peeled off using atraumatic forceps.

SC isolation

Fragments of ovarian cortex were digested using Liberase DH (Sigma-Aldrich, Bornem, Belgium) and DNase I (Roche Diagnostics, Brussels, Belgium), as previously described (Chiti *et al.*, 2017). The resulting cell suspension was halted by adding a similar volume of Dulbecco's phosphate-buffered saline (DPBS, Gibco, Paisley, UK) supplemented with 10% (v/v) heat-inactivated fetal bovine serum (FBS, Gibco, New York, USA) and 1% (v/v) antibiotic and antimycotic (Anti-Anti; Gibco, Bleiswijk, Netherlands). The cell suspension was then filtered through sterilized 80- and 30-µm nylon net filters (Millipore, Overijse, Belgium) (Soares *et al.*, 2015). The obtained solution was centrifuged at 1200 *g* for 10 min and the pellet was resuspended in DPBS plus 10% FBS for cell counting. A small proportion of isolated SCs (20%) from each ovarian biopsy were divided into two parts: (i) 15% were immediately fixed in 4% paraformaldehyde (VWR, Leuven, Belgium) for immunohistochemical analysis; (ii) 5% were snap-frozen for qPCR analysis. The rest was frozen for further *in vitro* culture.

Freezing and thawing of SC suspensions

The remaining 80% of SCs were centrifuged at 1200 *g* for 10 min and the pellet was resuspended in 1 ml DMEM/F12 supplemented with 20% FBS, 1% Anti-Anti and 10% dimethyl sulfoxide (Sigma-Aldrich). The cryovials were loaded into a Mr. Frosty™ freezing container (Thermo Fisher Scientific) and transferred to a −80°C freezer. After 24 h, cryovials were removed from the container and stored at −80°C till needed.

Once cells had been collected from eight patients, they were thawed for *in vitro* culture. For this, cryovials were kept for 2 min at 37 °C in a bead bath (Lab Armor, Cornelius, USA) and then the cell

suspension was transferred to 9 ml DMEM/F12. The diluted suspension was centrifuged at 1200 *g* for 10 min and supernatant was carefully removed. The remaining cell pellet was suspended in basic medium (BM) containing DMEM/F12 supplemented with 10% KnockOut™ serum replacement (KSR; Gibco) and 1% Anti-Anti. A total of 10 000 SCs were immediately fixed in 2.5% glutaraldehyde (Agar Scientific, Stansted, UK) in 0.1 M sodium cacodylate buffer (sodium salt trihydrate, 98% pure, Acros Organics, Thermo Fisher Scientific) for ultrastructural evaluation. Another group of 100 000 SCs were fixed in 4% paraformaldehyde for immunohistochemical analysis and 15 000 were snap-frozen for qPCR analysis. The remaining cells were divided into groups of 6×10^4 cells for *in vitro* culture.

SCs in *in vitro* culture

Since it was not possible to collect enough GCs from IVF patients, we replaced them by COV434 cells (ECACC 07071909; Culture Collections, Salisbury, UK) (Havelock *et al.*, 2004), which have been described as the best candidate to substitute GCs in follicle developmental studies (Zhang *et al.*, 2000). In order to mimic the follicle basement membrane that separates GCs from TCs, we used atelocollagen permeable inserts (Koken Co., Tokyo, Japan), as described by Orisaka *et al.* (2006).

Isolated SCs were cultured with or without COV434 cells using either BM or enriched medium (EM) (Supplementary Table SI) and seeded directly onto plastic or permeable atelocollagen inserts.

In total, four groups were created (Fig. 1):

G1—SCs in BM, seeded directly onto plastic dishes.

G2—SCs in EM, seeded directly onto plastic dishes.

G3—SCs in EM, seeded onto atelocollagen inserts.

G4—SCs co-cultured with 1.8×10^5 COV434 cells. In this group, COV434 cells were seeded onto one side of the atelocollagen inserts and, after 24 h of incubation at 37 °C with 5% CO_2, the inserts were inverted and the SCs were seeded onto the other side (Orisaka *et al.*, 2006).

For G1 and G2, 700 µl medium was added to the wells, while for G3 and G4, 300 µl medium was placed in the inserts and 400 µl in the wells. Half of the medium was changed every second day. For G4, half of the medium in the well (in direct contact with COV434 cells) and half from the insert (in direct contact with SCs) were separately collected and kept for analysis. Retrieved media were frozen at −20 °C for hormone measurement.

Cells were cultured for 8 days at 37 °C with 5% CO_2. It is important to note that in G1 and G2, apart from proliferating attached fibroblast-like cells, floating spheroid structures were also formed. They were removed from the wells when the medium was changed and, to avoid losing them, the medium was centrifuged at 1200 *g* for 10 min to collect the spheroids in the bottom of the tube and return them to their original dishes.

At the end of culture, the media were removed and frozen, and the SCs were detached using Accutase™ (Sigma-Aldrich). Cells were then counted and apportioned for qPCR (15% SCs), ultrastructural analysis (45% SCs) and immunohistochemistry (40% SCs).

RNA isolation and cDNA synthesis

SCs were snap-frozen before and after *in vitro* culture. They were treated with AllPrep DNA/RNA Micro Kit (Qiagen, Hilden, Germany) as described in the data sheet provided. In brief, cells were lysed with the Buffer RLT Plus supplied with the kit, passed through the DNA column, and then the liquid part was mixed with 70% ethanol following different centrifugation and washing steps in order to obtain purified RNA. To synthesize and amplify cDNA from a small RNA yield, the QuantiTect Whole Transcriptome Kit (Qiagen) was used. A gel electrophoresis method was applied to ensure the presence of synthesized cDNA.

qPCR analysis

To determine whether SCs are able to differentiate into TICs, relative mRNA levels for LH receptor (*Lhr*), steroidogenic acute regulatory protein (*Star*), cytochrome P450 17A1 (*Cyp11a1*), steroid 17-alpha-hydroxylase/17,20 lyase (*Cyp17a1*) and 3 beta hydroxysteroid dehydrogenase/delta 5–>4-isomerase types 1 (*Hsd3b1*) and 2 (*Hsd3b2*) were assessed in snap-frozen cells before and after *in vitro* culture. To this end, we used TaqMan probes (Applied Biosystems, Waltham, USA) for genes of interest (Supplementary Table SII), as well as the TaqMan Gene Expression Master Mix (Applied Biosystems) and diethyl pyrocarbonate-treated water (Thermo Fisher Scientific). To select the best housekeeping gene(s), samples from four different *in vitro* culture groups were loaded onto precoated TaqMan Array Human Endogenous Control Plates (Thermo Fisher Scientific) and qPCR was performed. Average expression stability of the investigated housekeeping genes was analyzed using the geNorm method in R, version 3.5.3.

Immunohistochemical analysis

Cytospin slides were prepared using isolated SCs fixed in paraformaldehyde before and after *in vitro* culture (G1 and G2), Superfrost Plus slides (Menzel-Glaser, Braunschweig, Germany) and a Thermo Electron Cytospin 2 centrifuge (Fisher Scientific, Brussels, Belgium) operating at 700 rpm for 5 min. Each cytospin slide contained approximately 30 000 cells.

Since we analyzed floating spheroid structures separately from attached cells, we named them F1 (and attached cells, G1) and F2 (and attached cells, G2). F1, F2, G3 and G4 were first fixed in 4% paraformaldehyde for 40 min at room temperature and then centrifuged at 1200 *g* for 10 min. After removing the supernatant, spheroid structures or cells were embedded in 30 µl of 2% UltraPure™ agarose (Invitrogen, Thermo Fisher Scientific) and centrifuged immediately at 14 000 *g* for 1 min to combine the spheroid structures/cells with the agarose. After solidification, the agarose mixture was dehydrated and embedded in paraffin. Five-µm-thick tissue sections were then placed on Superfrost Plus slides for immunohistochemical processing. The following markers were selected to assess SC differentiation into TCs: LHR, STAR, CYP11A1, CYP17A1, HSD3B1 and HSD3B2. We also added specific markers for TCs and small luteal cells: perilipin-2 (adipose differentiation-related protein (ADRP)), neurogenic locus notch homolog protein 1 (NOTCH1), aminopeptidase-N (CD13) and dipeptidyl peptidase IV (CD26) (Supplementary Table SIII).

Cytospin and paraffin-free slides were subjected to blocking of endogenous peroxidase activity by incubation in 3% H_2O_2 for 30 min. Antigen retrieval steps, antibody dilutions, incubation conditions and positive controls are summarized in Supplementary Table SIII. The primary antibody was omitted in negative controls and a mixture of

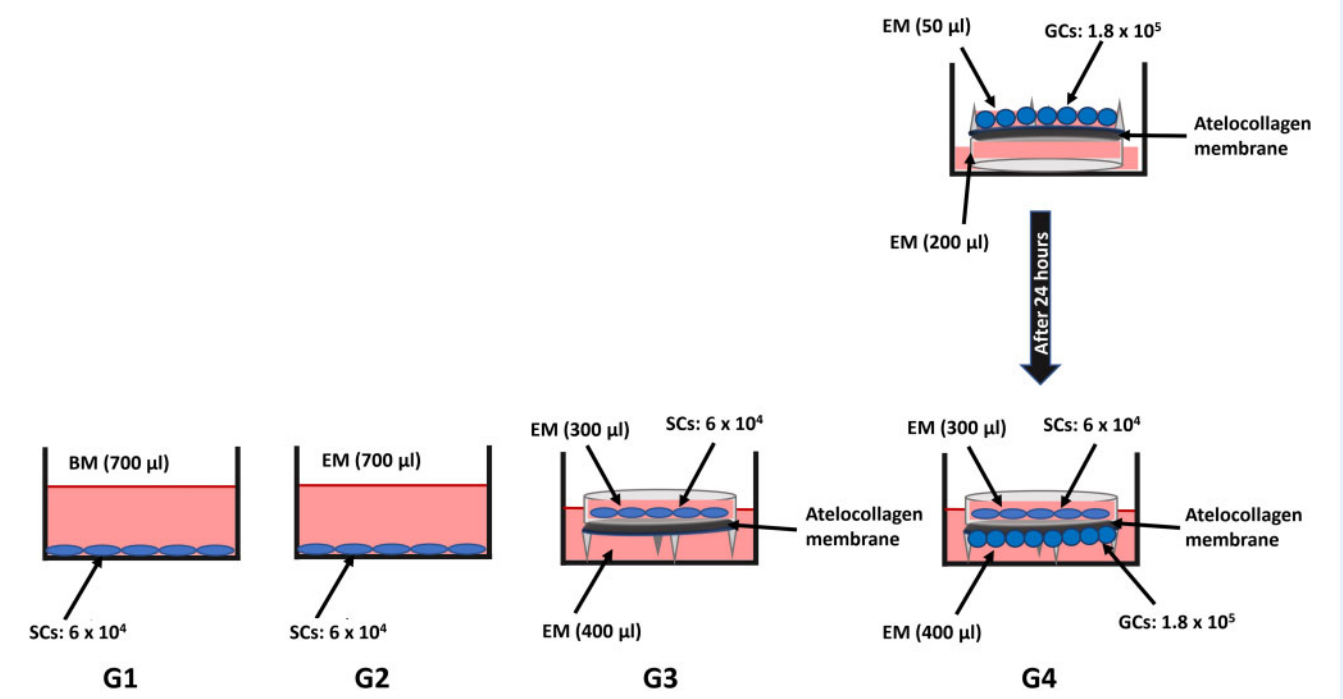

Figure 1. Schematic representation of the *in vitro* culture groups. G1: 6×10^4 SCs in basic medium (BM) containing DMEM-F12 supplemented with KSR and antibiotics, seeded directly onto a plastic dish. G2: 6×10^4 stromal cells (SCs) in enriched medium (EM) containing BM supplemented with growth factors, FSH and LH, seeded directly onto a plastic dish. G3: 6×10^4 SCs in EM seeded onto a permeable atelocollagen membrane. G4: 6×10^4 SCs in EM seeded onto the top of a permeable atelocollagen membrane in co-culture with 1.8×10^5 COV434 cells on the other side of the membrane.

FLEX universal negative control antibodies for rabbit or mouse was added (Dako, Glostrup, Denmark). Sections were stained with a solution of diaminobenzidine (Vector, Burlingame, USA), counterstained with hematoxylin, and mounted for light microscopy (Nikon Eclipse, Tokyo, Japan) analysis. Slides were visualized at 40× magnification and positive cells for each protein were counted by two independent observers.

Ultrastructural analysis

Cells fixed in glutaraldehyde before and after *in vitro* culture were washed in 0.2 M sodium cacodylate buffer (pH 7.4) and placed in 1% osmic acid (2% osmium tetraoxide solution, Carl Roth, Karlsruhe, Germany) and 0.1 M sodium cacodylate buffer solution for 1 hour. After a series of dehydration steps with ethanol, the cells were embedded in resin (Eponate 12, Ted Pella Inc., Redding, USA) and cut into 80-nm ultra-thin sections (Ultrotome III, LKB Company, Bromma, Sweden) using a diamond knife (Ultra 45°, Diatome Diamond Knives, Hatfield, USA). Ultra-thin sections were placed on a copper/rhodium grid (21-9M0300, Micro to Nano, Haarlem, the Netherlands). Samples were then contrasted with 2% uranyl acetate (Spi Supplies, West Chester, USA) in water, Reynold's lead nitrate (Millipore) and tris sodium citrate (VWR).

Hormone assays

Frozen media from each *in vitro* culture group were thawed for ELISA analysis at different time points (D2, D4, D6 and D8). Dehydroepiandrosterone (DHEA) and progesterone secreted by differentiated cells were measured using DHEA ELISA (ADI901093, Enzo Life Sciences BVBA, Farmingdale, USA) and progesterone ELISA (ADI900011, Enzo Life Sciences) kits.

Statistical analyses

All statistical analyses were performed using R, version 3.6.1. Because a number of genes (or proteins) were simultaneously assessed and multiple comparisons were carried out, *P*-values were adjusted for multiple testing using the Benjamini–Hochberg method to control the false discovery rate.

- qPCR: All transcriptomic data were analyzed using R, version 3.6.1. Before qPCR data analysis, the most stable housekeeping genes were selected from the dedicated dataset using the geNorm algorithm (Vandesompele *et al.*, 2002) implemented in the NormqPCR Bioconductor package. All undetected values were processed using the 'non-detects' Bioconductor package and imputed accordingly using an algorithm based on an expectation–maximization approach. Expression levels of each gene were then normalized according to the selected housekeeping genes by computing ΔCT values. The

Limma Bioconductor package was used to determine ΔΔCT values and associated *P*-values of each gene. This process was undertaken for each comparison and respective results were displayed in volcano plots.

- ELISA (DHEA and progesterone): For each element of interest, DHEA and progesterone levels were analyzed using linear mixed-effects models. Logarithmic transformation was applied to both DHEA and progesterone in order to normalize data distribution. In each model, the patient effect was assumed to follow normal distribution and was therefore defined as a random effect, while time was introduced as a fixed effect.
- Immunohistochemistry: Protein expression after *in vitro* culture was compared with D0 values using linear regression models.

Results

SCs isolated from ovarian tissue easily adhered to both plastic and permeable inserts after one day of *in vitro* culture. However, after two days, their appearance changed in G1 and G2, and spheroid structures started forming and floating in the medium (Fig. 2). It has been previously demonstrated that GCs and TCs cultured in serum-free conditions, reaggregate into multicellular clumps during *in vitro* culture, which indicates cell–cell or cell–extracellular matrix interactions (Yamada *et al.*, 1999; Yang and Xiong, 2012; Hatzirodos *et al.*, 2017). On Day 4, some fibroblast-like cells remained strongly attached to the plastic surface in G1 (Fig. 2), while almost all spheroid structures were detached from the bottom of the dish in G2 (Fig. 2). These structures continued to increase in diameter and became larger in G2 than in G1, with some measuring around 300 µm (Fig. 2). Conversely, cells in G3 and G4 remained adherent to the membrane throughout the *in vitro* culture period (Fig. 2). They exhibited typical fibroblast morphology and, after 8 days, entirely covered the inserts (Fig. 2).

Quantitative real-time polymerase chain reaction (qPCR)

Volcano plots of qPCR results from isolated SCs before and after *in vitro* culture revealed very different gene expression patterns for enzymes involved in the steroidogenic pathway of TICs, and special markers for TICs, such as *Lhr* and *Cyp17a1* (Fig. 3). In G1 (n = 5), a significant increase was observed in mRNA levels of *Cyp17a1* and *Hsd3b2* ($P < 0.05$). On the other hand, in F1 (n = 3), there was only an upturn in mRNA levels of *Cyp17a1* ($P < 0.05$). In G2 (n = 5), only *Hsd3b2* mRNA levels increased ($P < 0.05$), while in F2 (n = 3), *Lhr* mRNA levels rose significantly ($P < 0.05$) and *Hsd3b2* was on the verge of being significantly upregulated. In G3 (n = 3), *Hsd3b2* was upregulated ($P < 0.05$) and CYP11A1 and *Lhr* were both borderline in terms of significant upregulation, but in G4 (n = 8), mRNA levels of *Lhr* and *Hsd3b2* were both significantly upregulated ($P < 0.05$).

Immunohistochemical analysis

Results from protein expression of LHR, ADRP, STAR, CYP11A1, CYP17A1, HSD3B1, HSD3B2, NOTCH1, CD13 and CD26 were compared after 8 days of *in vitro* culture versus Day 0 (D0; control) (Table I).

It is important to point out that on D0, there was a considerable proportion of isolated SCs that were positive for LHCGR and HSD3B1, and more than 10% positive for CYP17A1 (Table I). Interestingly, after *in vitro* culture, there was increased expression of most proteins involved in the steroidogenic pathway in all groups (Table I; Figs 4 and 5). Apart from G1 and F1, all other groups exhibited a significant ($P < 0.05$) upturn in the number of CD13-positive cells (Table I; Fig. 4). Moreover, after *in vitro* culture, we observed a higher number of CD26-positive cells compared to controls (D0) (Table I; Fig. 5). There was also a significant increase ($P < 0.05$) in NOTCH1-positive cells in G3 and G4 (Table I, Fig. 5).

Expression of CD13, a specific marker for the theca interna with steroidogenic activity, is presented in Supplementary Fig. S1. Positive and negative control tissue and human ovary for each marker are shown in Supplementary Figs S2 and S3.

Ultrastructural analysis

Results from transmission electron microscopy (TEM) showed a remarkable difference between cells before and after *in vitro* culture and between groups. Before *in vitro* culture (D0), cells appeared to be undifferentiated, with a high nucleus/cytoplasm ratio, few organelles, mostly round mitochondria with scarce cristae (immature mitochondria) and few endoplasmic reticulum cisternae (Fig. 6, D0).

Different culture conditions did not appear to affect cell health status, as cells had a normal appearance, with some at the proliferative stage. In all groups, they developed an endoplasmic reticulum and showed higher numbers of mitochondria and lipid droplets compared to D0 (Figs 6, 7 and 8). Similar to D0 findings, cells in G1 and F1 had a high nucleus/cytoplasm ratio, and nuclei exhibited loose chromatin and visible nucleoli, suggesting DNA transcription (Fig. 6, G1-a). While we only found round mitochondria in F1 (Fig. 6, F1), we observed round and elongated mitochondria (Fig. 6, G1-c) and gap junctions between cells in G1 (Fig. 6, G1-b and c: arrow heads). In both G1 and F1, some endoplasmic reticulum and lipid droplets were detected in examined cells (Fig. 6, G1-b and F1).

In G2 (Fig. 6, G2-a) and F2 (Fig. 7, F2-a), we found active cells with a low nucleus/cytoplasm ratio. Ultrastructural analysis of attached cells (G2) showed that they had a round, oval or somewhat undulated nucleus, rough and abundant smooth endoplasmic reticulum, Golgi apparatus, lipid droplets, oval and elongated mitochondria with tubular or vesicular cristae and lysosomes (Fig. 6, G2-a; Fig. 7, G2-b and c). Ultrastructural analysis of F2 cells revealed that floating structures contained three different cell types (Fig. 7, F2-a): (i) cells with elongated nuclei, well developed rough endoplasmic reticulum, Golgi apparatus, rod-shaped mitochondria with lamellar cristae, lipid droplets and free ribosomes (Fig. 7, F2-a: circle); (ii) cells ellipsoidal in shape with an oval nucleus, rough endoplasmic reticulum, Golgi apparatus, lipid droplets, elongated or oval mitochondria with lamellar or tubular cristae, a fairly developed smooth endoplasmic reticulum and lysosomes (Fig. 7, F2-a: four tails star; Fig. 8, F2-e); and (iii) cells with the same ultrastructure as described for attached cells in G2 with undulated nuclei (Fig. 7, F2-a: five tails star, b, c and d).

Cells in G3 also proved to be active, with a low nucleus/cytoplasm ratio, nuclei with loose chromatin and visible nucleoli (one or two)

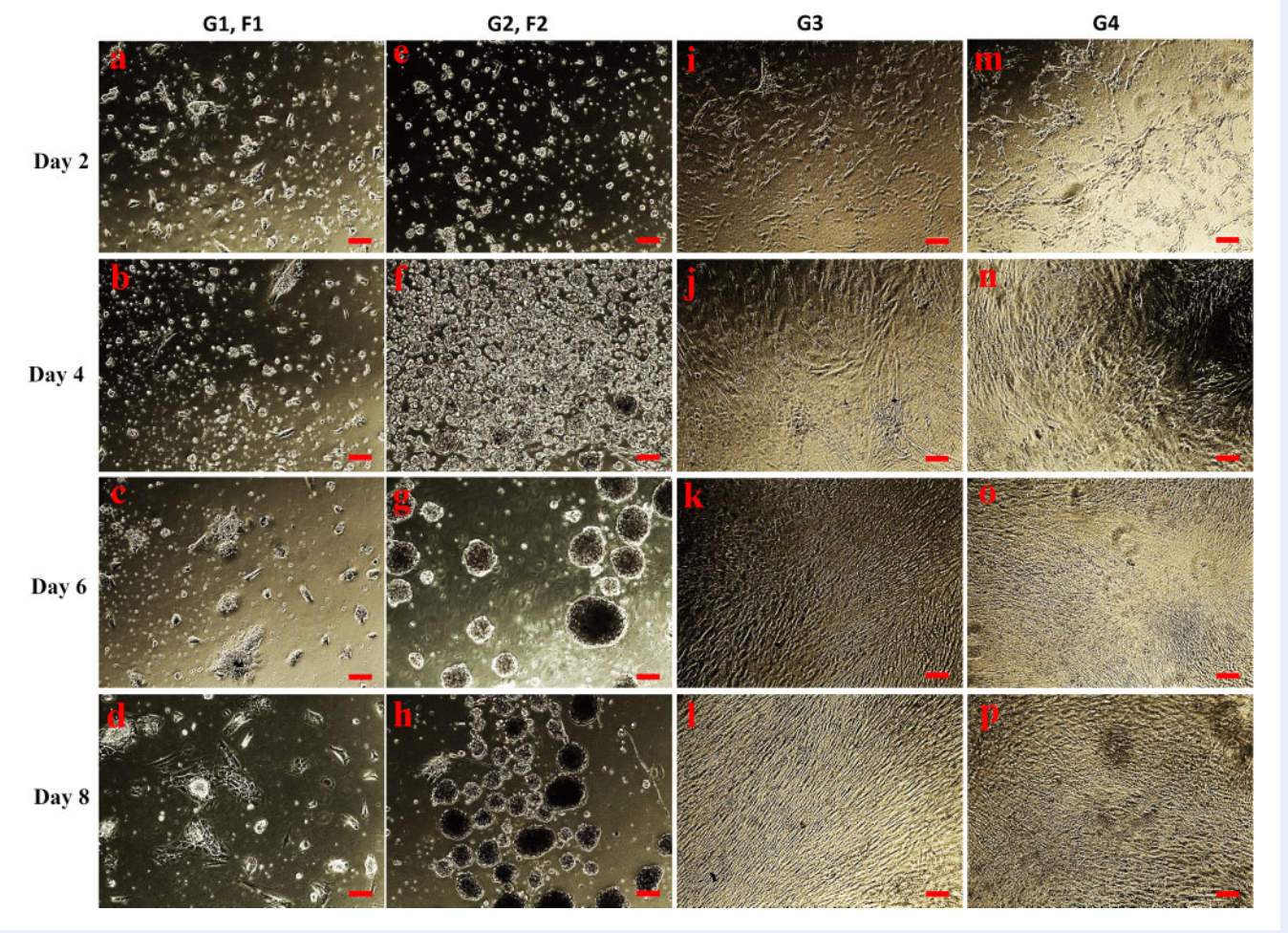

Figure 2. Stromal cells in *in vitro* culture. Ovarian cortical SCs in BM (G1, F1) at different time points (a, b, c, d). SCs in EM (G2, F2) at different time points (e, f, g, h). SCs in EM seeded onto an atelocollagen membrane (G3) at different time points (i, j, k, l). SCs in EM seeded onto one side of an atelocollagen membrane in co-culture with COV434 cells on the other side of the membrane (G4) at different time points (m, n, o, p). Scale bars: 100 μm. G1–G4 attached cells, F1, F2 floating cells.

(Fig. 8, G3-a). Ultrastructural evaluation of these cells showed cells similar to F2, but also the presence of a new cell type. This latter population presented with lamelliform microvilli, acentric nuclei, numerous lipid droplets, mitochondria with tubular cristae, well developed smooth and rough endoplasmic reticulum and Golgi apparatus (Fig. 8, G3-a and b).

G4 cells appeared to be less active than G3 cells, considering their low/medium nucleus/cytoplasm ratio (Fig. 8, G4-a). Their nuclei also showed loose chromatin and visible nucleoli (one or two) (Fig. 8, G4-a and b). Ultrastructural studies revealed the presence of a few cells similar to those found in F2, larger numbers of cells similar to G3, and a new group of cells with dense aggregates (Fig. 8, G4-c). Most cells in G4 exhibited an irregular rectangular shape with an eccentrically situated nucleus containing prominent nucleoli, mainly close to the nuclear membrane. Their Golgi apparatus had associated mitochondria, and they showed tubular endoplasmic reticulum, dense membrane-bound vesicular granules and many dense aggregates (Fig. 8, G4-a, b and c).

Secretion of DHEA and progesterone

Increasing patterns of secretion of DHEA and progesterone were observed by ELISA kits in different groups after 8 days of *in vitro* culture (Fig. 9). A linear trend was observed with time, showing a significant rise ($q < 0.001$) in DHEA concentrations in medium during the culture period in G1 ($n = 6$), G2 ($n = 5$), G3 ($n = 3$) and G4 ($n = 9$). A similar trend for progesterone levels also demonstrated a statistical increase ($q < 0.001$) in G2 ($n = 5$), G3 ($n = 3$) and G4 ($n = 9$), but G1 remained the same throughout the culture period. In co-culture conditions (G4), medium from the well, which was in contact with COV434 cells, contained no detectable amounts of DHEA or progesterone.

Statistical comparisons for progesterone levels between groups on Day 8 (D8) were as follows: G1 vs G2 ($q < 0.05$), G1 vs G3 ($q < 0.05$), G1 vs G4 ($q < 0.05$), G2 vs G3 ($q < 0.05$), G2 vs G4 ($q = 0.06$) and G3 vs G4 ($q = 0.22$).

Statistical comparisons for DHEA levels between groups on D8 were as follows: G1 vs G2 ($q = 0.33$), G1 vs G3 ($q = 0.09$), G1 vs G4

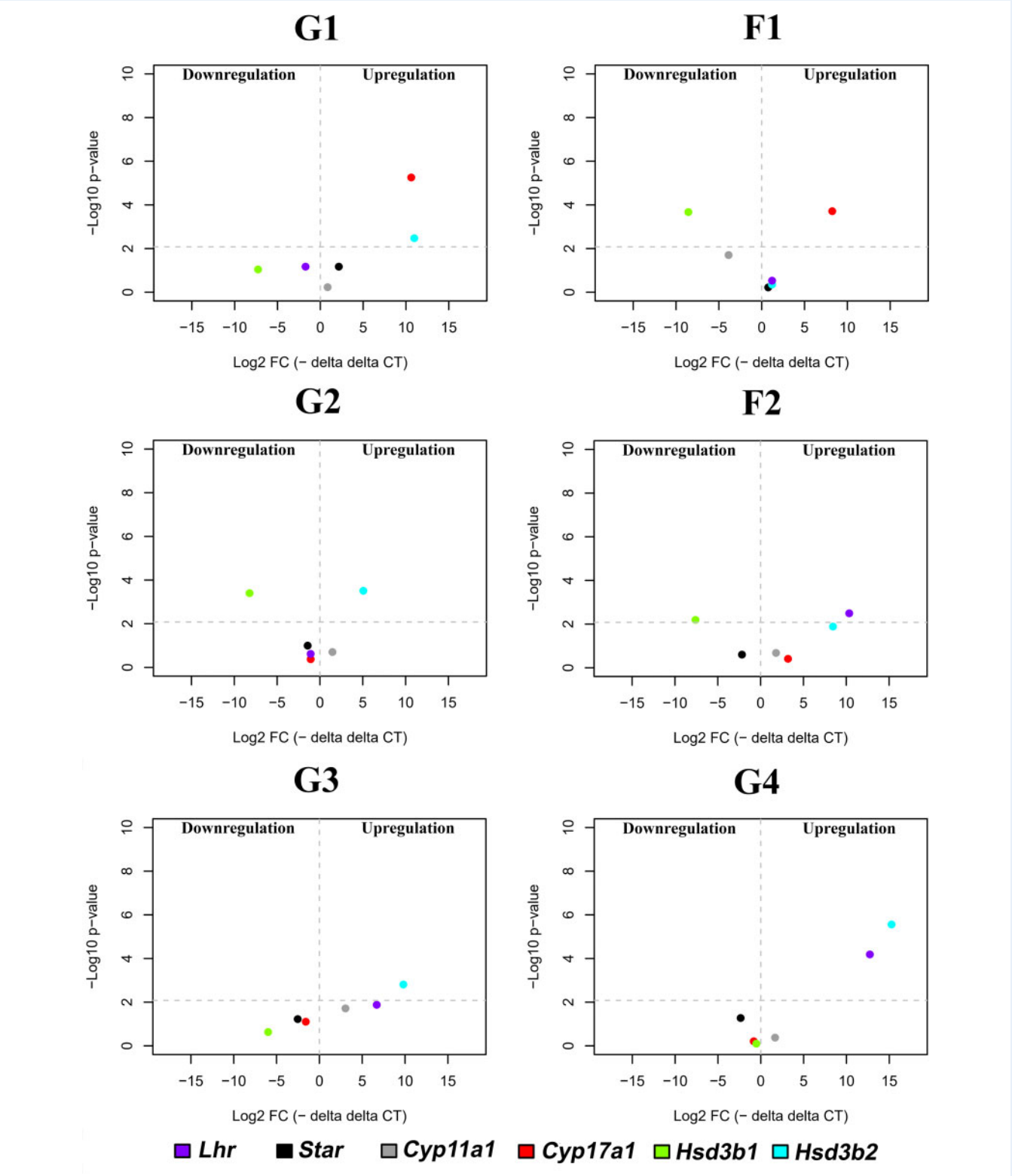

Figure 3. Quantitative real-time PCR results presented in volcano plots. mRNA expression for enzymes involved in steroidogenesis of theca/steroidogenic cells. Large magnitude fold changes (*x*-axis) and high statistical significance (-log10 of *P*-value, *y*-axis). The horizontal dashed line shows the position of $P = 0.05$, with dots above the line being $P < 0.05$ and dots below the line being $P > 0.05$. The vertical dashed line shows the boundary between down- and upregulation: downregulation on the left and upregulation on the right.

Table I Immunostaining of cells for different theca cell markers.

	Day 0	G1	F1	G2	F2	G3	G4
LHR	45.6%[a] (7481/16 397)	99%[b] (91/92)	36.1%[a] (129/357)		97.1%[b] (408/420)	90.5%[b] (247/273)	97.0%[b] (1156/1192)
STAR	0.2%[a] (1/570)	27%[b] (4/15)	82.2%[b] (693/758)		17.7%[b] (23/130)	6.3%[a] (78/1245)	26.8%[b] (82/306)
CYP11A1	0%[a] (0/331)	81.0[b] (191/236)	91.4%[b] (693/758)		99.1%[b] (114/115)	79.3%[b] (1153/1454)	97.5%[b] (2652/2720)
CYP17A1	16.7%[a] (139/833)	93.5%[b] (214/229)	64.1%[b] (397/619)	89%[b] (31/35)	79.0%[b] (729/923)	38.8%[a] (247/637)	99.4%[b] (2807/2823)
HSD3B1	47.5%[a] (95/200)	100%[b] (54/54)	98.8%[b] (163/165)		99.8%[b] (464/465)	98.9%[b] (178/180)	98.8%[b] (948/960)
HSD3B2	1.0%[a] (10/960)	74%[b] (29/39)	65.9%[b] (257/390)		24%[a] (20/85)	76.8%[b] (209/272)	94.8%[b] (346/365)
ADRP	0%[a] (0/1400)	93%[b] (51/55)	88.3%[b] (293/332)		99.2%[b] (124/125)	93.3%[b] (265/284)	97.7[b] (469/480)
CD13	0%[a] (0/10)	0%[a] (0/36)	1.6%[a] (6/377)	43%[b] (30/77)	21.1%[b] (76/360)	33.8%[b] (67/198)	24.5%[b] (111/453)
CD26	5.2%[a] (11/213)	47%[a] (34/72)	93.8%[b] (180/192)	100%[b] (10/10)	84.1%[b] (269/320)	76.5%[b] (130/170)	98.2%[b] (933/950)
NOTCH1	0.5%[a] (3/580)	4%[a] (2/47)	24.1%[a] (63/261)		12.2%[a] (22/181)	92.1%[b] (557/605)	95.6%[b] (717/750)

For each staining protocol values show mean percentage of positively stained cells (numbers in parentheses show number of positive cells out of the total number of cells counted).
[a,b]Indicate the statistical difference ($P < 0.05$) in each group after 8 days culture compared to Day 0 for every immunostaining.
ADRP, adipose differentiation-related protein; CD13, aminopeptidase-N; CD26, dipeptidyl peptidase IV; CYP11A1, cholesterol side-chain cleavage enzyme; CYP17A1, cytochrome P450 17A1; D0, Day 0; HSD3B1, hydroxy-delta-5-steroid dehydrogenase, 3 beta- and steroid delta-isomerase 1; HSD3B2, hydroxy-delta-5-steroid dehydrogenase, 3 beta- and steroid delta-isomerase 2; LHR, luteinizing hormone receptor; NOTCH1, Notch homolog 1, translocation-associated (drosophila); STAR, steroidogenic acute regulatory protein.

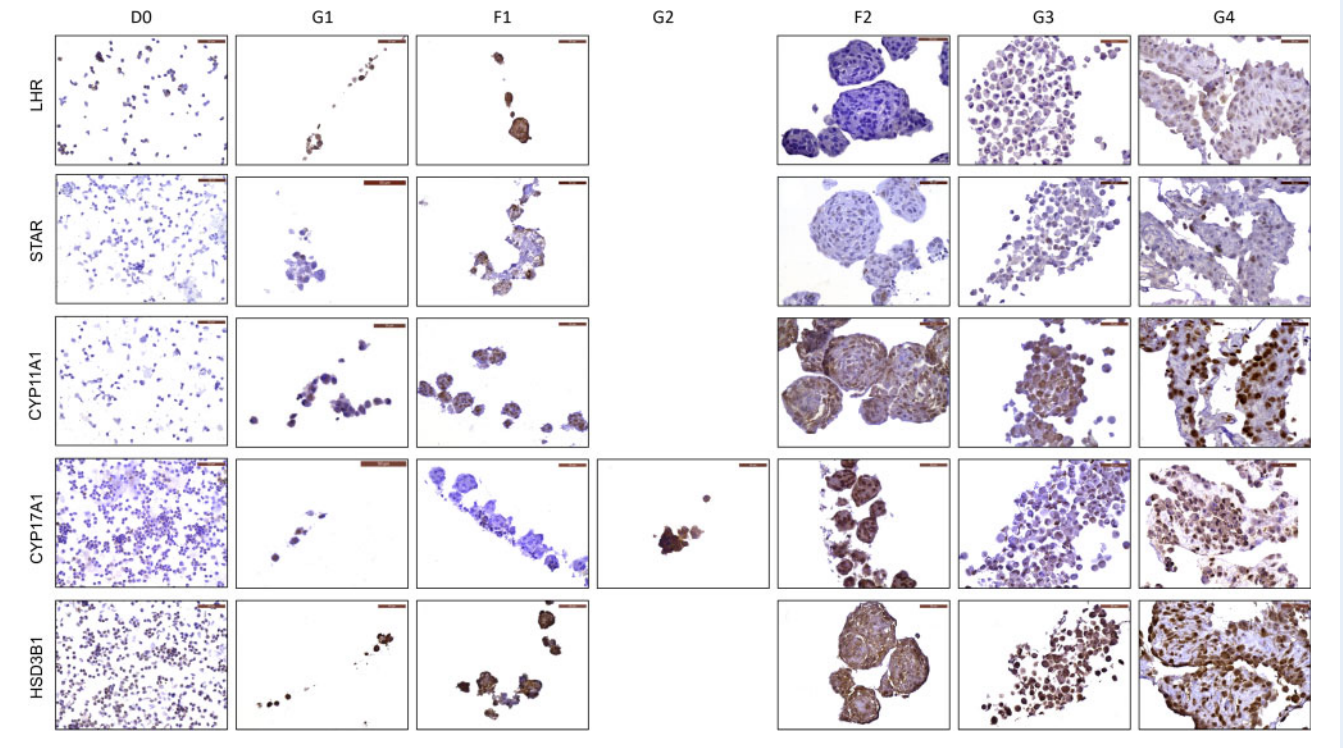

Figure 4. Immunohistochemistry of LHR, STAR, CYP11A1, CYP17A1 and HSD3B1 in cells on D0 (before culture), and G1, F1, G2, F2, G3 and G4 after 8 days of *in vitro* culture. Scale bars: 50 μm.

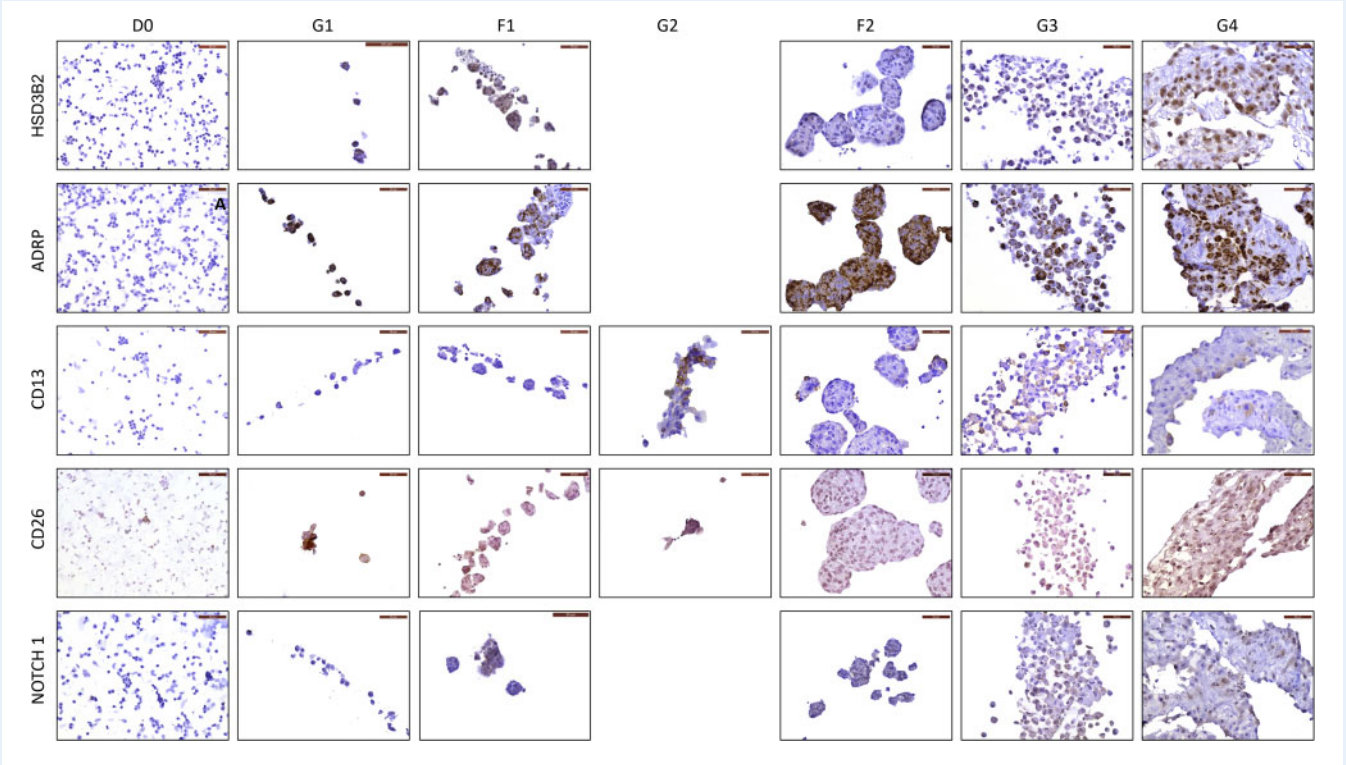

Figure 5. Immunohistochemistry of HSD3B2, ADRP, CD13, CD26 and NOTCH1 in cells on D0 (before culture), and G1, F1, G2, F2, G3 and G4 after 8 days of *in vitro* culture. Scale bars: 50 µm.

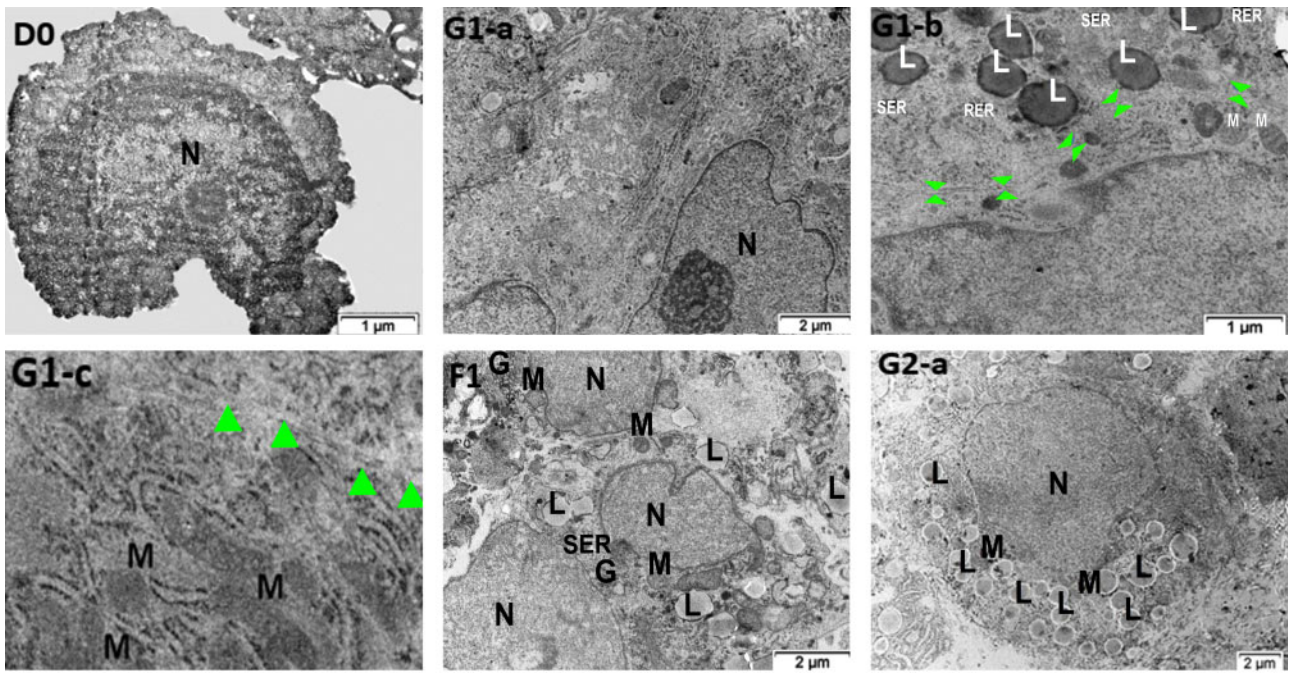

Figure 6. Transmission electron microscopy of cells before (D0) and after 8 days of *in vitro* culture. Cells before *in vitro* culture (D0). Ovarian cortical SCs in BM showing attached cells at the bottom of the well (G1—a, b and c) and floating spheroid structures (F1). SCs in EM showing attached cells at the bottom of the well (G2-a). G, Golgi apparatus; L, lipid droplets; M, mitochondria; N, nucleus; RER, rough endoplasmic reticulum; SER, smooth endoplasmic reticulum. G1-b and c: arrow heads: gap junctions.

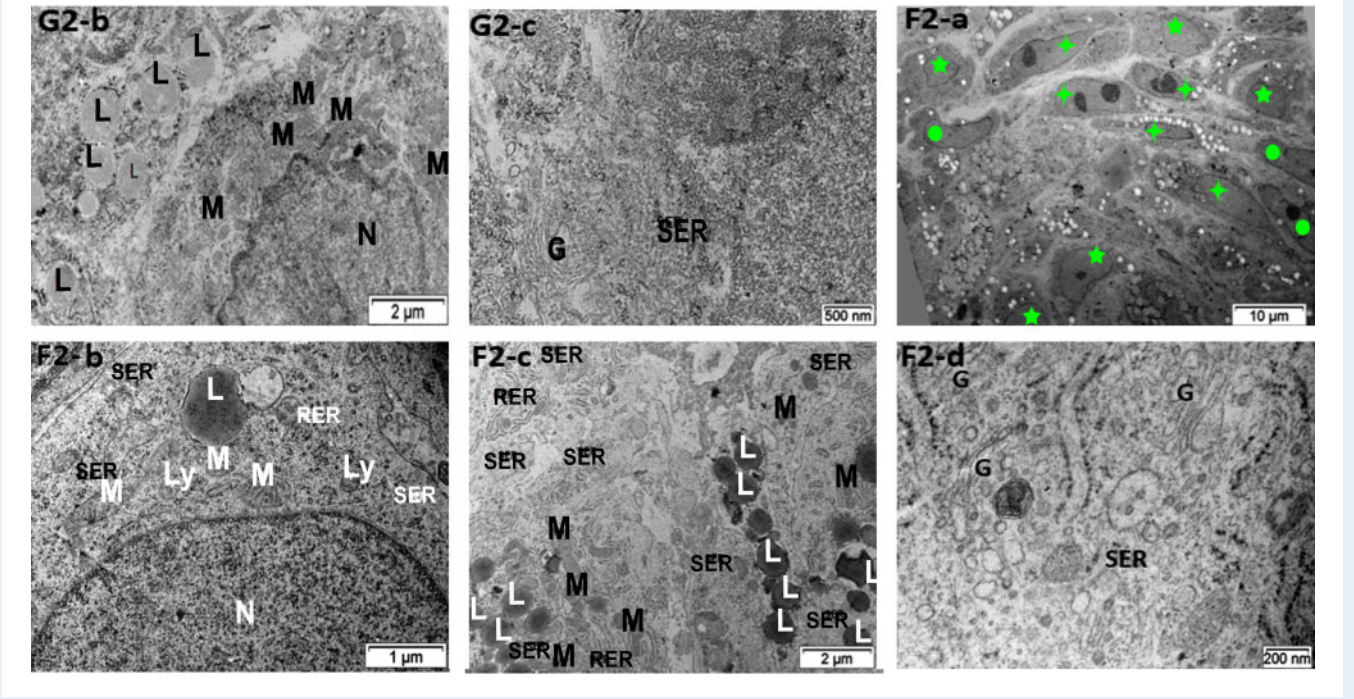

Figure 7. Transmission electron microscopy of cells after 8 days of *in vitro* culture. Ovarian cortical SCs in EM showing attached cells at the bottom of the well (G2—b and c) and floating spheroid structures (F2—a, b, c and d). Ly, lysosome. F2-a: circle: fibroblast; four tails star: transitional cells; five tails star: theca cells.

($q = 0.09$), G2 vs G3 ($q = 0.47$), G2 vs G4 ($q = 0.58$) and G3 vs G4 ($q = 0.58$).

Discussion

Since the main goal of our experiments was to obtain differentiated human TCs, we designed a study where we *in vitro*-cultured SCs isolated from the cortical layer of postmenopausal ovaries in medium enriched with growth factors thought to be involved in TC differentiation (Honda *et al.*, 2007; Liu *et al.*, 2015; Dalman *et al.*, 2018a,b). Since GCs have also been implicated in this process, we tested the co-culture approach with GCs (Orisaka *et al.*, 2006; Qiu *et al.*, 2013) as well. In all tested groups, we obtained large numbers of steroid-producing cells. At first, gene and protein expression patterns for proteins involved in the theca steroidogenic pathway appeared to indicate that virtually all cortical ovarian cells can differentiate into TCs, which would be in line with findings obtained in studies using bovine and caprine SCs (Orisaka *et al.*, 2006; Qiu *et al.*, 2013). However, in G1, the lack of CD13 immunostaining, a surface marker specific to TCs (Fujiwara *et al.*, 1992), showed that these cells were not TCs. On the other hand, ultrastructural analysis and the presence of CD13-positive cells confirmed that the TC population accounted for 21–43% of differentiated cells in the other groups (G2, G3 and G4). Interestingly, differentiation was not found to halt once cells were converted into TCs. In fact, just like in the human ovary, this process advances until TC luteinization and small luteal cell senescence, as evidenced by TEM. With the help of atelocollagen inserts, which improved cell attachment and proliferation and consequently their communication, TC differentiation was faster, so small luteal cells could be detected (G3 and G4). Addition of COV434 cells accelerated this process further, as older luteal cells with aggregates of luteal debris were also observed in G4. Luteal debris consists of small, dense, circular elements representing clumps of regressing luteal cells, as described by Fraser *et al.* (1999) and Adams and Hertig (1969).

G1 and F1 were both significantly positive for *Cyp17a1* mRNA and all studied proteins involved in the steroidogenic pathway. TEM images from the two different cell populations in the first group (G1 and F1) showed characteristics of steroid-producing cells: they were positive for all enzymes involved in the steroidogenic pathway and CD26, but negative for CD13 and NOTCH1. mRNA expression is not always consistent with the level of expressed proteins. The correlation can be as little as 40%, depending on the tissue and *in vitro* culture system (Vogel and Marcotte, 2012). There are many processes between transcription and translation and, as mentioned by Vogel and Marcotte (2012), protein stability is a big factor. The half-life of different proteins can range from minutes to days, while the degradation rate of mRNA would fall within a much tighter range (2–7 h for mammalian mRNA vs 48 h for protein) (Vogel and Marcotte, 2012). Moreover, the ultrastructure of these cells was different from TCs in the ovaries, which show steroid-secreting activity and are characterized by a round, oval or somewhat undulated nucleus, Golgi apparatus, rough endoplasmic reticulum, abundant smooth endoplasmic reticulum, lipid droplets, oval mitochondria with tubular or vesicular cristae and lysosomes

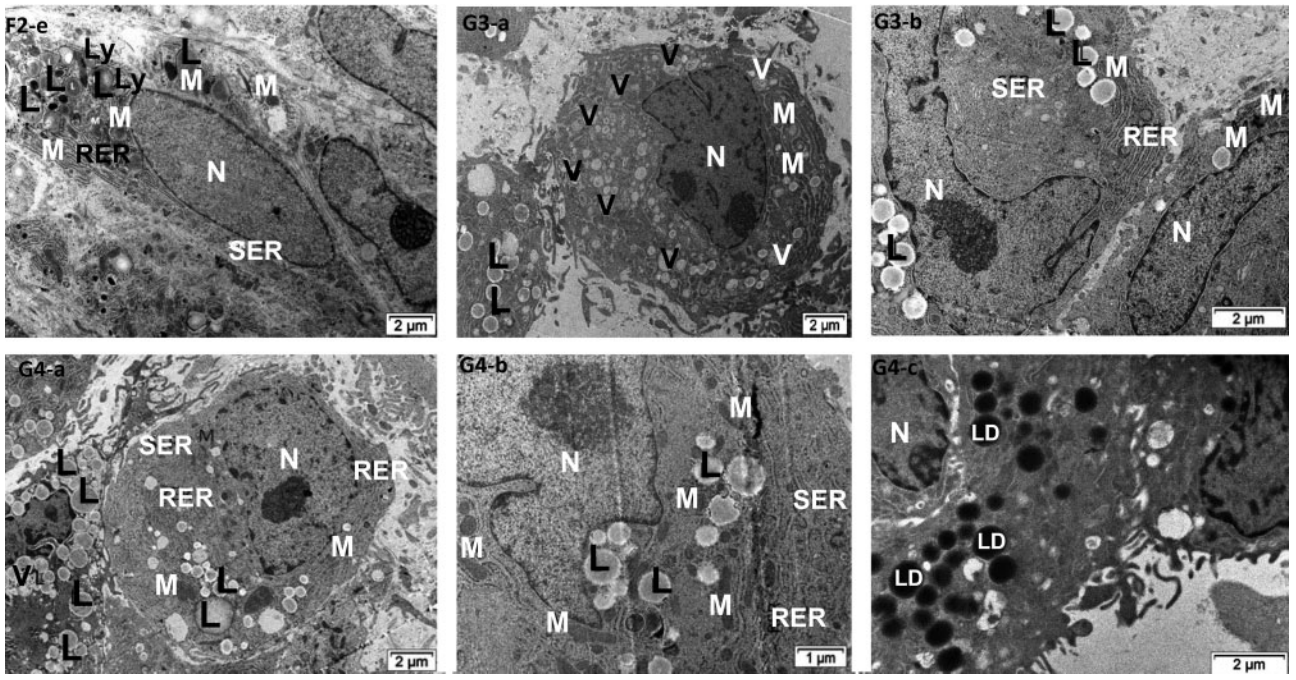

Figure 8. Transmission electron microscopy of cells after 8 days of *in vitro* culture. Floating spheroid structures (F2-e), ovarian cortical SCs in EM seeded onto an atelocollagen membrane (G3—a and b), and SCs in EM seeded onto one side of an atelocollagen membrane in co-culture with COV434 cells on the other side of the membrane (G4—a, b and c). LD, luteal debris; V, vacuole.

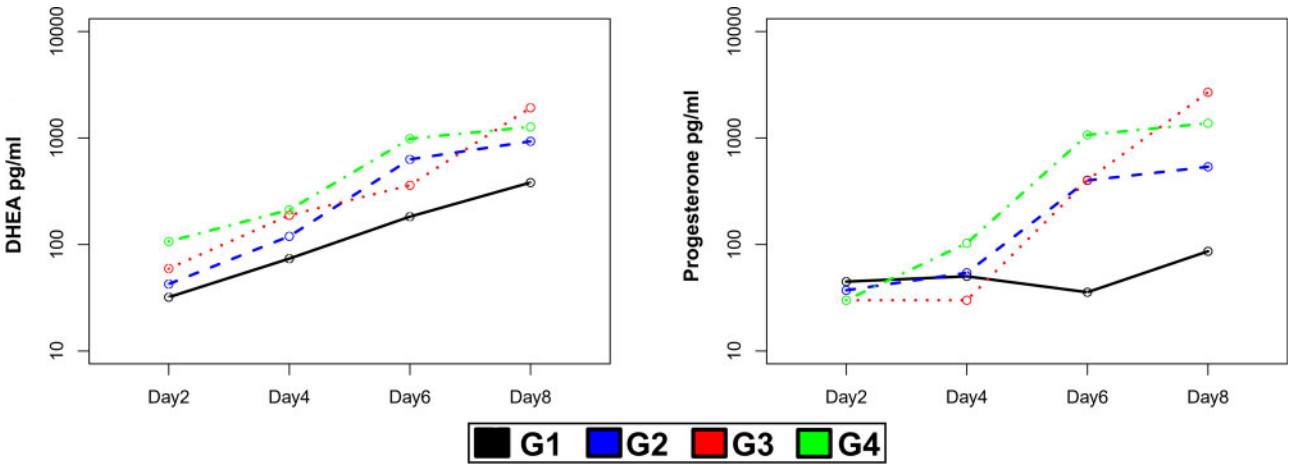

Figure 9. Enzyme-linked immunosorbent assays. Dehydroepiandrosterone levels on the left and progesterone levels on the right. Different time points for hormone measurement in the *x*-axis and logarithmic expression of hormones (pg/ml) in the *y*-axis. SCs in BM (G1). SCs in EM (G2) at different time points, SCs in EM seeded onto an atelocollagen membrane (G3) at different time points, SCs in EM seeded onto one side of an atelocollagen membrane in co-culture with COV434 cells on the other side of the membrane (G4) at different time points.

(Hiura *et al.*, 1981). On the other hand, the presence of gap junctions in attached cells in G1 and increasing secretion patterns of DHEA but not progesterone during *in vitro* culture are reported to be specific characteristics of ovarian interstitial steroid-producing cells (Dawson and McCabe, 1951; Semenova, 1969). According to Erickson *et al.* (1985), there are four types of interstitial cells in the ovary: primary (Gondos and Hobel, 1973), secondary (Kingsbury, 1939; Dawson and McCabe, 1951), theca (Peters, 1969) and hilar (Semenova, 1969).

Differentiation observed in G1 could be due to KSR, which contains mainly lipid-rich albumin (Kojima et al., 2016), and these lipids could be responsible for DHEA synthesis. Indeed, in murine testicular explant culture, KSR was shown to increase testosterone production (Reda et al., 2017). DHEA is the precursor of testosterone in testes and androstenedione in ovarian TCs (Bordini and Rosenfield, 2011).

Since TCs differentiate adjacent to developing follicles, it is assumed that once follicles start their growth, they secrete factors that stimulate TC differentiation (Magoffin and Magarelli, 1995; Honda et al., 2007; Liu et al., 2015). Ovarian interstitial cells develop and maintain a specialized phenotype in serum-free conditions, which is different from other types of cells in the ovary. It is clear that LH is the most important stimulating force in interstitial cells, inducing their differentiation both at morphological and biochemical levels (Erickson et al., 1985). In addition to LH, there are other major factors that affect TC differentiation (Honda et al., 2007). Using neonatal mouse ovaries, Honda et al. (2007) showed that purified putative theca stem cells were induced to differentiate into TCs *in vitro* under the influence of LH, IGF-1, SCF (also known as kit ligand), and conditioned medium from GCs. IGF-1 alone stimulated expression of LHRs (Magoffin and Weitsman, 1994) and steroidogenic enzymes. CYP11A1 and HSD3B, but not CYP17A1, was found to act synergistically with LH to increase expression of these enzymes (Magoffin and Weitsman, 1993a,b,c). In rats, a combination of IGF-1 and SCF increased expression of LHR, STAR, CY11A1, CYP17A1 and HSD3B, which provides strong evidence that these factors may act synergistically to regulate TC differentiation and steroid production (Huang et al., 2001). bFGF has been shown to impact somatic cell mitosis, steroid synthesis, differentiation and apoptosis (Walters and Schallenberger, 1984; Tilly et al., 1992; Lavranos et al., 1994), while may influence theca development indirectly through stimulating SCF expression (Nilsson and Skinner, 2004). TGF-β superfamily members like bone morphogenetic proteins and growth differentiation factors, with vital roles in controlling follicle growth and development (Shimasaki et al., 2004; Knight and Glister, 2006; Xia and Schneyer, 2009), are also involved in TC recruitment, proliferation and differentiation, which may or may not interact with gonadotropins (Young and McNeilly, 2010). By enriching the medium with growth factors purportedly involved in this process, as well as FSH and LH, we observed much lower concentrations of attached fibroblast-like cells and larger spheroid structures in G2 than in G1. Steroidogenic ultrastructural features of attached G2 cells and their undulated nucleus appeared to indicate that they had differentiated into TCs. Moreover, their membrane stained positive for CD13. ELISA results confirmed that these cells were actively secreting steroids; there was an increase in DHEA production from Day 2 (D2), while progesterone secretion started after four days of *in vitro* culture.

F2 structures were upregulated for *Lhr* and *Hsd3b2* and also expressed proteins and enzymes involved in the steroidogenic pathway of TCs. Ultrastructurally, these cells have three distinct features; some of them are fibroblast-like cells (Kingsbury, 1939) with elongated nuclei, others are transitional cells (Kingsbury, 1939) ellipsoidal in shape with an oval nucleus, and a further group resembles TCs with an undulated nucleus (Hiura et al., 1981). Transitional cells are found halfway along the differentiation pathway of fibroblasts into TCs (Kingsbury, 1939).

Interestingly, our results from G2 and F2 show that being attached to a surface promoted a faster differentiation, demonstrating that substrate also has an impact on cell behavior (Kanta, 2015). This was confirmed in G3, where all cells remained firmly attached to the collagen membrane and differentiation reached the last stage, namely small luteal cells. Cells in G3 showed upregulation of *Lhr*, *Cyp11a1* and *Hsd3b2* at the mRNA level and expressed steroidogenic enzymes and CD13, CD26 and NOTCH1. Indeed, the ultrastructure of these cells showed the presence of small concentrations of fibroblasts, transitional cells and TCs and a large number of small luteal cells (Van Lennep and Madden, 1965), with lamelliform microvilli and an acentric nucleus together with other characteristics of steroidogenic cells (Ohara et al., 1987). Our ELISA results show higher levels of secreted DHEA and progesterone in G3 medium compared to G2. Moreover, increasing DHEA levels from Day 2 of *in vitro* culture (D2) and progesterone secretion from Day 4 (D4) onwards also support our findings.

In G4, cells exhibited upregulated mRNA levels of *Lhr*, *Cyp11a1* and *Hsd3b2* and were positive for proteins and enzymes involved in the steroidogenic pathway of TCs, plus the three markers of steroidogenic/theca and luteal cells, CD13, CD26 and NOTCH1. Ultrastructural analysis revealed the presence of a few fibroblasts, transitional cells and TCs (Hiura et al., 1981). However, most cells were ultrastructurally similar to small luteal cells. Conversely, luteal cells obtained from this group were somewhat different from luteal cells from G3, as they contained luteal debris, resembling older small luteal cells (Dawson and McCabe, 1951; Enders, 1962; Enders and Lyons, 1964; Green and Maqueo, 1965; Van Lennep and Madden, 1965; Blanchette, 1966; Adams and Hertig, 1969). We also observed a profuse agranular endoplasmic reticulum together with mitochondria containing tubular cristae, which is characteristic of many types of actively secreting steroid cells, including active human corpora lutea (Green and Maqueo, 1965; Van Lennep and Madden, 1965) and small luteal cells in different mammalian species (Enders, 1962; Enders and Lyons, 1964; Blanchette, 1966). According to Adams and Hertig (1969), a close association between tubular endoplasmic reticulum and mitochondria may be a morphological reflection of the conversion of cholesterol to progesterone.

Apart from growth factors, hormones and substrate, the presence of a GC line also plays a role in cell differentiation. Indeed, COV434 cells accelerate cell differentiation even further, as demonstrated by the presence of older small luteal cells with aggregates of luteal debris. Honda et al. (2007) also reported that while medium enriched with growth factors and hormones did lead to cell differentiation, fully mature TCs were only obtained after co-culture with GCs. It would be interesting to perform COV434 cell co-culture with BM in order to gain a better understanding of the role of GCs in TC differentiation.

Due to the similarity between bovine and human ovaries, we hypothesized that cortical SCs in general could differentiate into TCs (Orisaka et al., 2006). However, we observed that while most cells became steroidogenic after *in vitro* culture, only a proportion of them were TCs, which indicates that there is a population of precursor TCs in human ovaries as in mouse ovaries (Liu et al., 2015). More interestingly, such cells remain in human ovaries, even after menopause. Recently, Fan et al. (2019) showed a number of genes expressed by progenitor TCs, including NME2, APOD, APOC1, MEST, WFDC1, MATN2, PTCH1 and ACTA2 in the theca layer of antral follicles. In their study on progenitor TCs, Dalman et al. (2018a,b) differentiated theca stem cells from human small antral follicles and reported LHR, GLI2 and PTCH1 as markers of these cells. Since all these studies

were conducted in the theca layer where cells already received differentiation signals, further studies are needed to confirm the presence of progenitor TCs in fertile and postmenopausal human ovaries. The introduced markers could help to test the hypothesis of progenitor TCs and serve to identify these cells in postmenopausal ovaries.

In conclusion, we showed for the first time that human TCs can differentiate *in vitro* under the influence of different growth factors and hormones (Honda *et al.*, 2007; Liu *et al.*, 2015; Dalman *et al.*, 2018a,b). These cells closely resemble their ovarian counterparts when investigated by immunohistochemical, ultrastructural and functional analyses. Our results are a great step forward in the understanding of TC ontogenesis in human ovaries. Moreover, *in vitro*-generated human TCs can be used for studies on drug screening and exposure to endocrine-disrupting chemicals, as well as elucidating TC-associated pathologies, such as androgen-secreting tumors and polycystic ovary syndrome.

Supplementary data

Supplementary data are available at *Human Reproduction* online.

Data availability

The datasets generated and analysed during the current study are available from the corresponding author on reasonable request.

Acknowledgements

We are grateful to Mira Hryniuk for reviewing the English language of the manuscript and Dolores Gonzalez and Olivier Van Kerk for their technical assistance. We also thank Prof. Carolina M. Lucci (University of Brasília, Brazil) for her advice during cell ultrastructure analysis and all patients who donated ovarian tissue for research.

Authors' roles

P.A.: study design, experimental procedures, analysis, interpretation of data and manuscript preparation. M.M.D.: tissue supply and manuscript revision. J.A.: statistical analysis. A.C.: support for analysis of ultrastructural images. C.A.A.: experimental design, experimental procedures, interpretation of results and manuscript revision.

Funding

This study was supported by grants from the Fonds National de la Recherche Scientifique de Belgique (FNRS) (C.A.A. is an FRS-FNRS Research Associate; grant MIS #F4535 16 awarded to C.A.A.; grant 5/4/150/5 awarded to M.M.D.; grant ASP-RE314 awarded to P.A.) and Foundation Against Cancer (grant 2018-042 awarded to A.C.).

Conflict of interest

The authors declare no conflict of interests.

References

Adams EC, Hertig AT. Studies on the human corpus luteum. I. Observations on the ultrastructure of development and regression of the luteal cells during the menstrual cycle. *J Cell Biol* 1969;**41**:696–715.

Adib S, Valojerdi MR. Molecular assessment, characterization, and differentiation of theca stem cells imply the presence of mesenchymal and pluripotent stem cells in sheep ovarian theca layer. *Res Vet Sci* 2017;**114**:378–387.

Blanchette EJ. Ovarian steroid cells: II. The lutein cell. *J Cell Biol* 1966;**31**:517–542.

Bordini B, Rosenfield RL. Normal pubertal development: Part I: the endocrine basis of puberty. *Pediatr Rev* 2011;**32**:223–229.

Chiti MC, Dolmans M-M, Hobeika M, Cernogoraz A, Donnez J, Amorim CA. A modified and tailored human follicle isolation procedure improves follicle recovery and survival. *J Ovarian Res* 2017;**10**:71.

Dalman A, Totonchi M, Valojerdi MR. Establishment and characterization of human theca stem cells and their differentiation into theca progenitor cells. *J Cell Biochem* 2018a;**119**:9853–9865.

Dalman A, Totonchi M, Valojerdi MR. Human ovarian theca-derived multipotent stem cells have the potential to differentiate into oocyte-like cells *in vitro*. *Cell J* 2018b;**20**:527–536.

Dawson AB, McCabe M. The interstitial tissue of the ovary in infantile and juvenile rats. *J Morphol* 1951;**88**:543–571.

Edson MA, Nagaraja AK, Matzuk MM. The mammalian ovary from genesis to revelation. *Endocr Rev* 2009;**30**:624–712.

Enders AC. Observations on the fine structure of lutein cells. *J Cell Biol* 1962;**12**:101–113.

Enders AC, Lyons W. Observations on the fine structure of lutein cells: II. The effects of hypophysectomy and mammotrophic hormone in the rat. *J Cell Biol* 1964;**22**:127–141.

Erickson GF, Magoffin DA, Dyer CA, Hofeditz C. The ovarian androgen producing cells: a review of structure/function relationships. *Endocr Rev* 1985;**6**:371–399.

Fan X, Bialecka M, Moustakas I, Lam E, Torrens-Juaneda V, Borggreven N, Trouw L, Louwe L, Pilgram G, Mei H. Single-cell reconstruction of follicular remodeling in the human adult ovary. *Nature Commun* 2019;**10**:1–13.

Fraser H, Lunn S, Harrison D, Kerr JB. Luteal regression in the primate: different forms of cell death during naturaland gonadotropin-releasing hormone antagonist or prostaglandin analogue-induced luteolysis. *Biol Reprod* 1999;**61**:1468–1479.

Fujiwara H, Maeda M, Imai K, Fukuoka M, Yasuda K, Horie K, Takakura K, Taii S, Mori T. Differential expression of aminopeptidase-N on human ovarian granulosa and theca cells. *J Clin Endocrinol Metab* 1992;**74**:91–95.

Gondos B, Hobel C. Interstitial cells in the human fetal ovary. *Endocrinology* 1973;**93**:736–739.

Green JA, Maqueo M. Ultrastructure of the human ovary: I. The luteal cell during the menstrual cycle. *Am J Obstet Gynecol* 1965;**92**:946–957.

Hatzirodos N, Glister C, Hummitzsch K, Irving-Rodgers HF, Knight PG, Rodgers RJ. Transcriptomal profiling of bovine ovarian granulosa and theca interna cells in primary culture in comparison with their *in vivo* counterparts. *PLoS One* 2017;**12**:e0173391.

Havelock JC, Rainey WE, Carr BR. Ovarian granulosa cell lines. *Mol Cell Endocrinol* 2004;**228**:67–78.

Hiura M, Nogawa T, Fujiwara A. Electron microscopy of cytodifferentiation and its subcellular steroidogenic sites in the theca cell of the human ovary. *Histochemistry* 1981;**71**:269–277.

Honda A, Hirose M, Hara K, Matoba S, Inoue K, Miki H, Hiura H, Kanatsu-Shinohara M, Kanai Y, Kono T *et al.* Isolation, characterization, and *in vitro* and *in vivo* differentiation of putative thecal stem cells. *Proc Natl Acad Sci USA* 2007;**104**:12389–12394.

Huang CT, Weitsman SR, Dykes BN, Magoffin DA. Stem cell factor and insulin-like growth factor-I stimulate luteinizing hormone-independent differentiation of rat ovarian theca cells. *Biol Reprod* 2001;**64**:451–456.

Itami S, Yasuda K, Yoshida Y, Matsui C, Hashiura S, Sakai A, Tamotsu S. Co-culturing of follicles with interstitial cells in collagen gel reproduce follicular development accompanied with theca cell layer formation. *Reprod Biol Endocrinol* 2011;**9**:159.

Kanta J. Collagen matrix as a tool in studying fibroblastic cell behavior. *Cell Adh Migr* 2015;**9**:308–316.

Kingsbury B. Atresia and the interstitial cells of the ovary. *Am J Anat* 1939;**65**:309–331.

Knight PG, Glister CJR. TGF-B superfamily members and ovarian follicle development. *Reproduction* 2006;**132**:191–206.

Kojima K, Sato T, Naruse Y, Ogawa T. Spermatogenesis in explanted fetal mouse testis tissues. *Biol Reprod* 2016;**95**:63.

Lavranos TC, Rodgers HF, Bertoncello I, Rodgers RJ. Anchorage-independent culture of bovine granulosa cells: the effects of basic fibroblast growth factor and dibutyryl camp on cell division and differentiation. *Exp Cell Res* 1994;**211**:245–251.

Liu C, Peng J, Matzuk MM, Yao HH-C. Lineage specification of ovarian theca cells requires multicellular interactions via oocyte and granulosa cells. *Nat Commun* 2015;**6**:1–11.

Magoffin DA, Magarelli PC. Preantral follicles stimulate luteinizing hormone independent differentiation of ovarian theca-interstitial cells by an intrafollicular paracrine mechanism. *Endocr* 1995;**3**:107–112.

Magoffin DA, Weitsman SR. Effect of insulin-like growth factor-I on cholesterol side-chain cleavage cytochrome p450 messenger ribonucleic acid expression in ovarian theca-interstitial cells stimulated to differentiate *in vitro*. *Mol Cell Endocrinol* 1993a;**96**:45–51.

Magoffin DA, Weitsman SR. Insulin-like growth factor-I stimulates the expression of 3 beta-hydroxysteroid dehydrogenase messenger ribonucleic acid in ovarian theca-interstitial cells. *Biol Reprod* 1993b;**48**:1166–1173.

Magoffin DA, Weitsman SR. Differentiation of ovarian theca-interstitial cells *in vitro*: regulation of 17 alpha-hydroxylase messenger ribonucleic acid expression by luteinizing hormone and insulin-like growth factor-I. *Endocrinology* 1993c;**132**:1945–1951.

Magoffin DA, Weitsman SR. Insulin-like growth factor-I regulation of luteinizing hormone (LH) receptor messenger ribonucleic acid expression and LH-stimulated signal transduction in rat ovarian theca-interstitial cells. *Biol Reprod* 1994;**51**:766–775.

Nilsson EE, Skinner MK. Kit ligand and basic fibroblast growth factor interactions in the induction of ovarian primordial to primary follicle transition. *Mol Cell Endocrinol* 2004;**214**:19–25.

Ohara A, Mori T, Taii S, Ban C, Narimoto K. Functional differentiation in steroidogenesis of two types of luteal cells isolated from mature human corpora lutea of menstrual cycle. *J Clin Endocrinol Metab* 1987;**65**:1192–1200.

Orisaka M, Tajima K, Mizutani T, Miyamoto K, Tsang BK, Fukuda S, Yoshida Y, Kotsuji F. Granulosa cells promote differentiation of cortical stromal cells into theca cells in the bovine ovary. *Biol Reprod* 2006;**75**:734–740.

Peters H. The development of the mouse ovary from birth to maturity. *Eur J Endocrinol* 1969;**62**:98–116.

Qiu M, Liu J, Han C, Wu B, Yang Z, Su F, Quan F, Zhang Y. The influence of ovarian stromal/theca cells during *in vitro* culture on steroidogenesis, proliferation and apoptosis of granulosa cells derived from the goat ovary. *Reprod Dom Anim* 2014;**49**:170–176.

Qiu M, Quan F, Han C, Wu B, Liu J, Yang Z, Su F, Zhang Y. Effects of granulosa cells on steroidogenesis, proliferation and apoptosis of stromal cells and theca cells derived from the goat ovary. *J Steroid Biochem Mol Biol* 2013;**138**:325–333.

Reda A, Albalushi H, Montalvo SC, Nurmio M, Sahin Z, Hou M, Geijsen N, Toppari J, Söder O, Stukenborg J-B. Knock-out serum replacement and melatonin effects on germ cell differentiation in murine testicular explant cultures. *Ann Biomed Eng* 2017;**45**:1783–1794.

Semenova I. Adrenergic innervation of ovaries in Stein-Leventhal syndrome. *Vestn Akad Med Nauk SSSR* 1969;**24**:58–62.

Shimasaki S, Moore RK, Otsuka F, Erickson GF. The bone morphogenetic protein system in mammalian reproduction. *Endocr Rev* 2004;**25**:72–101.

Soares M, Sahrari K, Chiti MC, Amorim C, Ambroise J, Donnez J, Dolmans M-M. The best source of isolated stromal cells for the artificial ovary: medulla or cortex, cryopreserved or fresh? *Hum Reprod* 2015;**30**:1589–1598.

Tilly JL, Billig H, Kowalski KI, Hsueh A. Epidermal growth factor and basic fibroblast growth factor suppress the spontaneous onset of apoptosis in cultured rat ovarian granulosa cells and follicles by a tyrosine kinase-dependent mechanism. *Mol Endocrinol* 1992;**6**:1942–1950.

Van Lennep EW, Madden LM. Electron microscopic observations on the involution of the human corpus luteum of menstruation. *Z Zellforsch Mikrosk Anat* 1965;**66**:365–380.

Vandesompele J, De Preter K, Pattyn F, Poppe B, Van Roy N, De Paepe A, Speleman F. Accurate normalization of real-time quantitative RT-PCR data by geometric averaging of multiple internal control genes. *Genome Biol* 2002;**3**:RESEARCH0034.

Vitt UA, McGee EA, Hayashi M, Hsueh AJ. *In vivo* treatment with GDF-9 stimulates primordial and primary follicle progression and theca cell marker CYP17 in ovaries of immature rats. *Endocrinology* 2000;**141**:3814–3820.

Vogel C, Marcotte EM. Insights into the regulation of protein abundance from proteomic and transcriptomic analyses. *Nat Rev Genet* 2012;**13**:227–232.

Walters DL, Schallenberger E. Pulsatile secretion of gonadotrophins, ovarian steroids and ovarian oxytocin during the periovulatory phase of the oestrous cycle in the cow. *J Reprod Fertil* 1984;**71**:503–512.

Xia Y, Schneyer AL. The biology of activin: recent advances in structure, regulation and function. *J Endocrinol* 2009;**202**:1–12.

Yamada S, Fujiwara H, Honda T, Higuchi T, Nakayama T, Inoue T, Maeda M, Fujii S. Human granulosa cells express integrin α2 and collagen type IV: possible involvement of collagen type IV in granulosa cell luteinization. *Mol Hum Reprod* 1999;**5**:607–617.

Yang Z, Xiong H-R. *Culture Conditions and Types of Growth Media for Mammalian Cells Biomedical Tissue Culture*. Croatia: InTech, 2012, 3–18.

Young J, McNeilly AS. Theca: the forgotten cell of the ovarian follicle. *Reproduction* 2010;**140**:489–504.

Zhang H, Vollmer M, De Geyter M, Litzistorf Y, Ladewig A, Dürrenberger M, Guggenheim R, Miny P, Holzgreve W, De Geyter C. Characterization of an immortalized human granulosa cell line (COV434). *Mol Hum Reprod* 2000;**6**:146–153.